Supporting information

Molten Salt Mediated Synthesis of Graphene-based Electrode from Low-Concentration Methane for Enhanced Oxygen Evolution Reaction

Zeai Huang ,*[abc] Tong Liu,[b] Ruiyang Zhang,[ab] Junjie Zhan,[b] Mingkai Yang,[b] Kuikui Zhang,[b] Yunxiao Zhou,[b] Chao Duan,[b] Guoxing Chen [d] and Ying Zhou *[abc]

[a] State Key Laboratory of Oil and Gas Reservoir Geology and Exploitation, Southwest Petroleum University, Chengdu, 610500, China

[b] School of New Energy and Materials, Southwest Petroleum University, Chengdu, 610500, China

[c] Sichuan-Chongqing Joint Key Laboratory of Green Hydrogen Production & Storage and Efficient Utilization, Southwest Petroleum University, Chengdu, 610500, China

[d] Department of Materials and Earth Sciences, Technical University Darmstadt, Darmstadt, 64287, Germany

S.1 Schematic diagram of graphene production from methane pyrolysis to electrode fabrication.

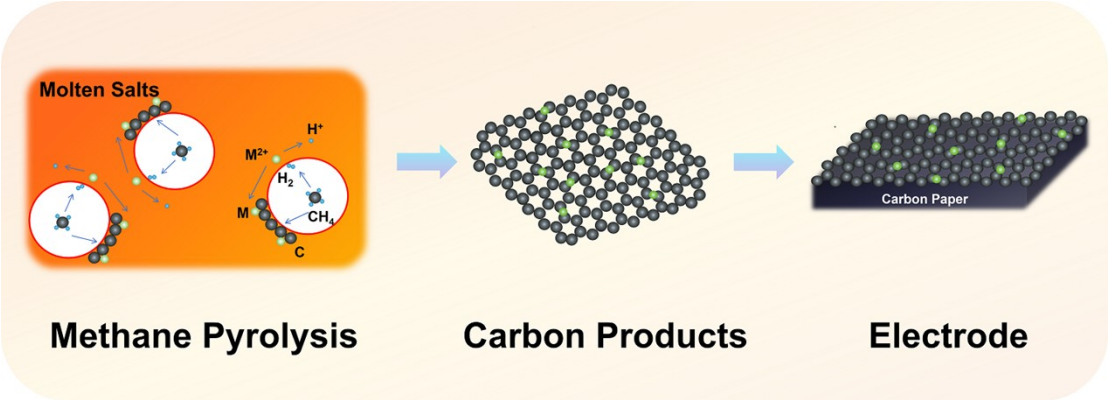

Fig. S1 Schematic diagram of graphene production from methane pyrolysis to electrode fabrication.

In the molten salt medium, methane gas continuously decomposes to produce carbon and hydrogen gas. The hydrogen gas further reduces M^{2+} ions in the melt salt to metal M, which is then embedded into the surface of the carbon material. The Ni^{2+} ions are reduced to metallic Ni, which activates the C-H bonds in methane by providing surface atomic sites with low coordination numbers. These sites can effectively adsorb and dissociate methane molecules. For instance, Mona A. Abdel-Fatah et al. also found that hydrocarbons adsorb and decompose on the active surface of nickel catalysts at high temperatures, triggering carbon formation.[1, 2] Using a slurry coating method, these copper and nickel-containing carbon materials are coated onto carbon paper, resulting in the fabrication of working electrodes for OER activity testing (Fig. S1).

S.2 AFM image of C-Cu6/Ni6.

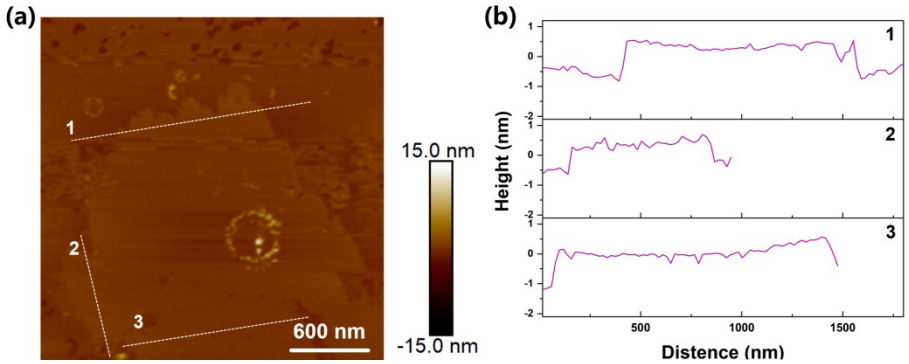

Fig. S2 AFM image of C-Cu6/Ni6.

S.3 Atomic percentages of Cu and Ni elements in carbon products from different groups.

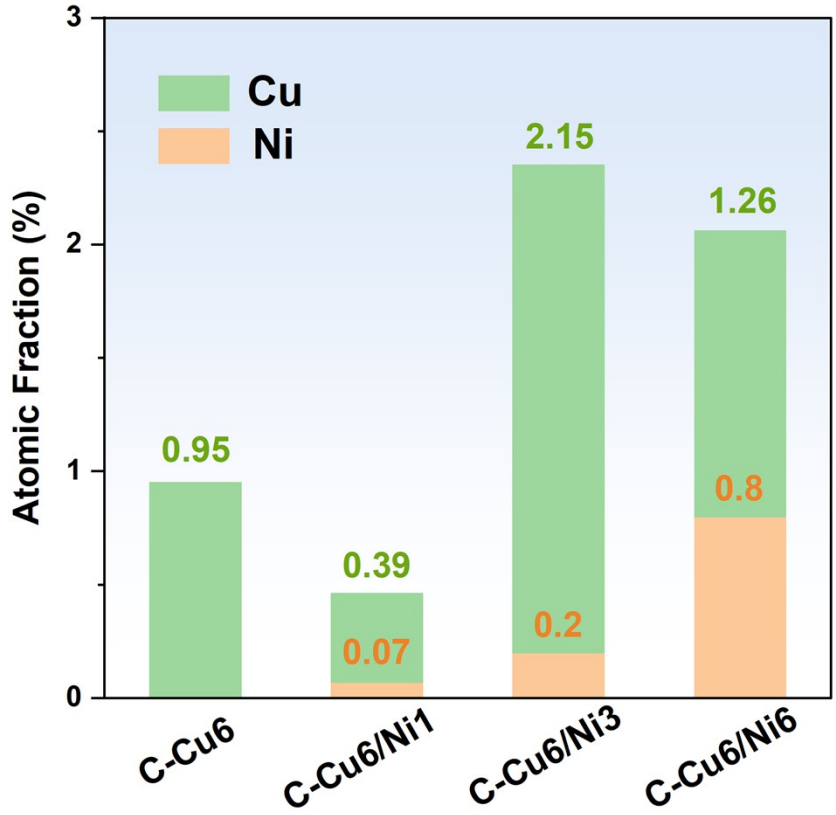

Fig. S3 Atomic percentages of Cu and Ni elements in carbon products from different groups.

S.4 XPS Spectra of C 1s for C-Cu6/Ni1 and C-Cu6/Ni3 Catalysts

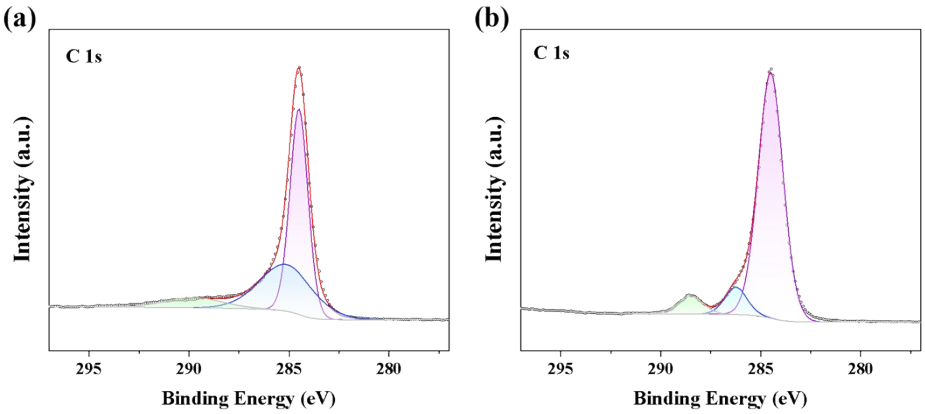

Fig. S4 XPS C 1s Spectrum: (a) C-Cu6/Ni1; (b) C-Cu6/Ni3.

S.5 XRD patterns of various carbon products

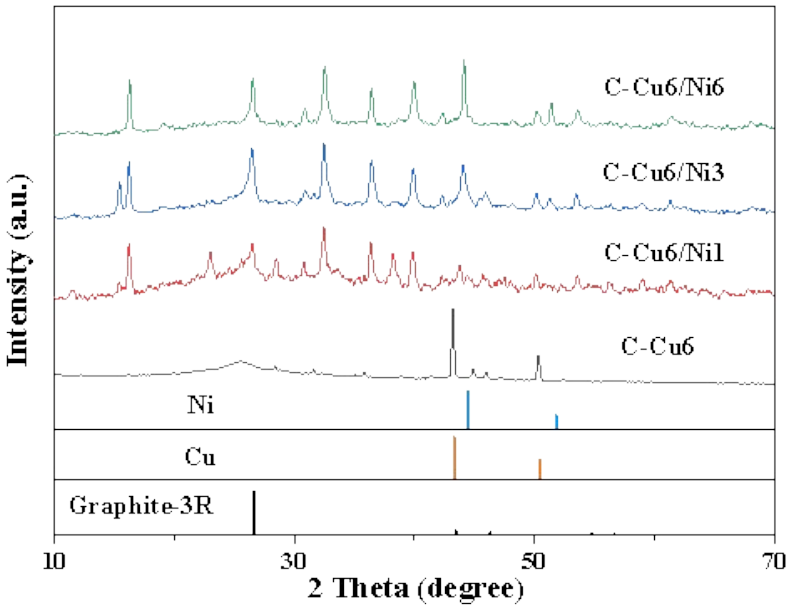

Fig. S5 XRD patterns of various carbon products.

S.6 SEM images of the electrodes prepared from various carbon products.

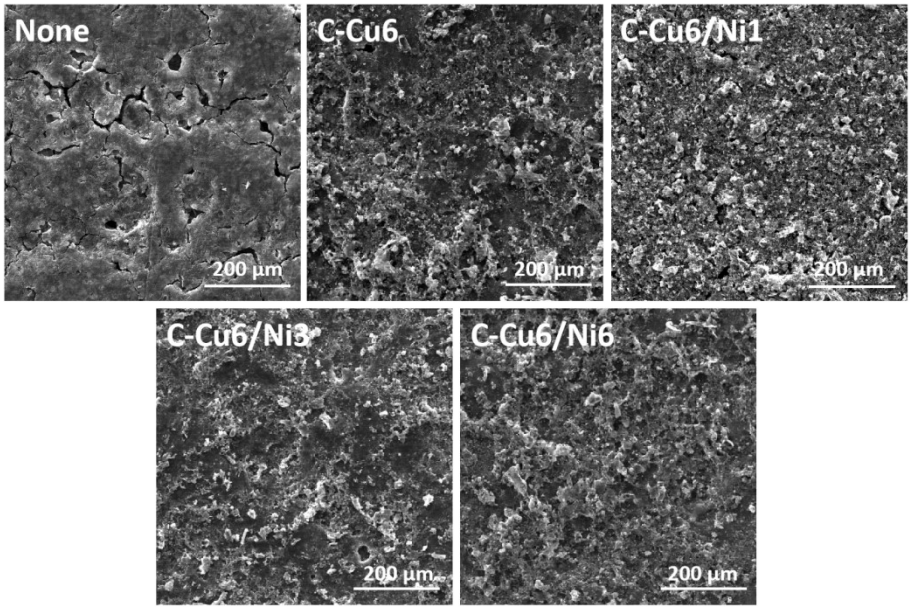

Fig. S6 SEM images of blank carbon paper and electrodes prepared from various carbon products.

S.7 XRD pattern of the cleaned Cu6/Ni6 material.

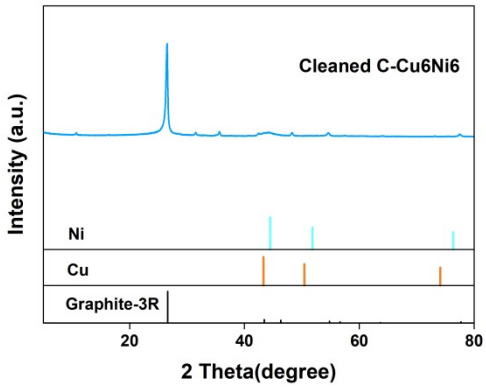

Fig. S7 XRD pattern of the cleaned Cu6/Ni6 material.

S.8 The LSV and Tafel curves of Cu6, Cu6/Ni6, and Cleaned Cu6/Ni6 electrodes..

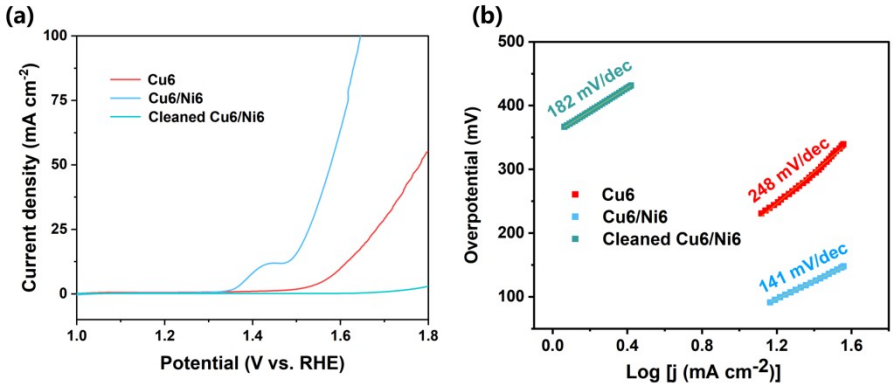

Fig. S8 (a) LSV curves of Cu6, Cu6/Ni6, and Cleaned Cu6/Ni6 electrodes, (b) Tafel curves of Cu6, Cu6/Ni6, and Cleaned Cu6/Ni6 electrodes.

The OER test was conducted on the C-Cu6Ni6 material after cleaning, and it was named Cleaned Cu6/Ni6. As shown in Fig. S7, the peak of Cu in the cleaned C-Cu6/Ni6 sample has disappeared, indicating that Cu has been completely removed by cleaning, while the peak of Ni still exists, suggesting that Ni remains in the sample. The LSV curve (Fig. S8a) shows that Cleaned Cu6/Ni6 requires a higher potential to reach the same current density compared with the original Cu6/Ni6 and Cu6 samples, which indicates that the presence of Cu has a positive effect on OER activity. The Tafel plot (Fig. S8b) shows that the Tafel slope of

Cleaned Cu6/Ni6 lies between Cu6/Ni6 and Cu6. The lower the Tafel slope, the higher the intrinsic activity of the electrocatalyst, thus confirming the importance of Ni doping in enhancing OER activity. In summary, Ni and Cu have a synergistic effect in improving the activity of the oxygen evolution reaction. The synergistic effect between Ni and Cu is also demonstrated in previous work.[3]

S.9 The CV cyclic curves and C_{dl} extraction results of Cu6/Ni6 and Cleaned Cu6/Ni6 electrodes.

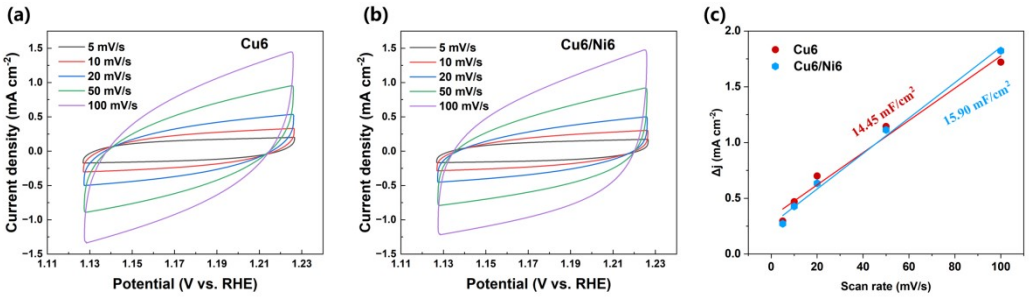

Fig. S9 (a) CV cyclic curves of Cu6/Ni6 and Cleaned Cu6/Ni6 electrodes, (b) C_{dl} extraction results of Cu6/Ni6 and Cleaned Cu6/Ni6 electrodes.

Cyclic voltammetry (CV) tests were performed on Cu6 and Cu6/Ni6 electrodes.As shown in Fig. S9, the electrochemical active surface area (ECSA) was determined based on the Cdl values. The ECSA of Cu6/Ni6 is slightly higher than that of Cu6. After normalization, the normalized exchange current densities ($J_{0,\ normalized}$) of Cu6 and Cu6/Ni6 are 4.48 μA cm^{-2} and 8.28 μA cm^{-2}, respectively. The $J_{0,\ normalized}$ of the Cu6/Ni6 sample is about 85% higher than that of the Cu6 sample, indicating a significantly higher intrinsic activity. The higher ECSA value also means that more active sites are fully exposed. Overall, the excellent catalytic performance of the Cu6/Ni6 sample is attributed to the synergistic effect of its structural advantages and intrinsic activity.[4-6]

S.10 Long-term stability test of the Cu6/Ni6 electrode.

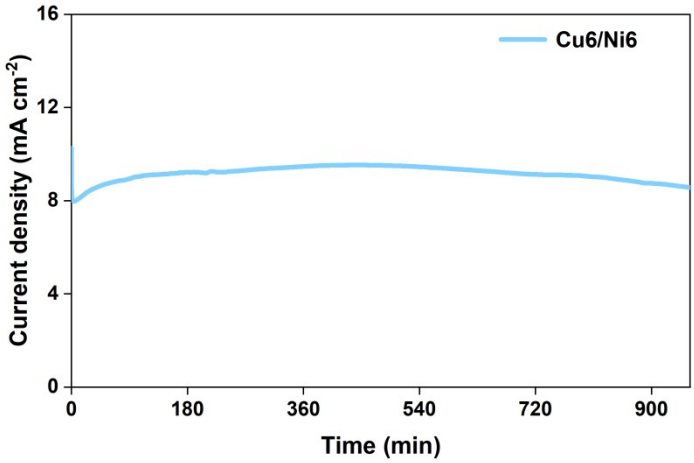

Fig. S10 Long-term stability test of the Cu6/Ni6 electrode.

The long - term performance of the Cu6/Ni6 electrode was evaluated. Under constant - potential operation, the corresponding current density of 10 mA cm^{-2} was highly stable over a period of 960 min(as shown in Fig. S10).

S.11 XPS spectra of the Cu6/Ni6 electrode before and after the reaction.

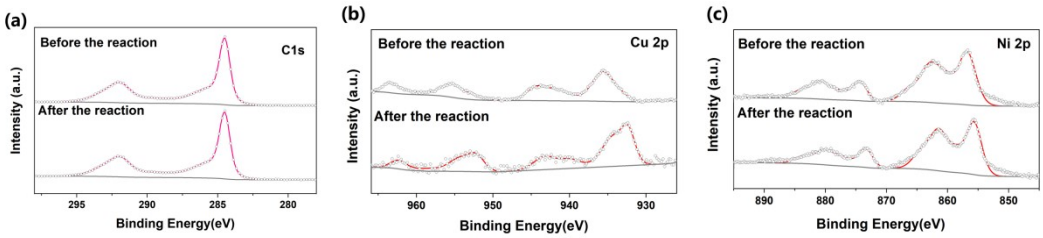

Fig. S11 XPS spectra of the Cu6/Ni6 electrode before and after the reaction.

S.12 SEM images of the Cu6/Ni6 electrode before and after the reaction.

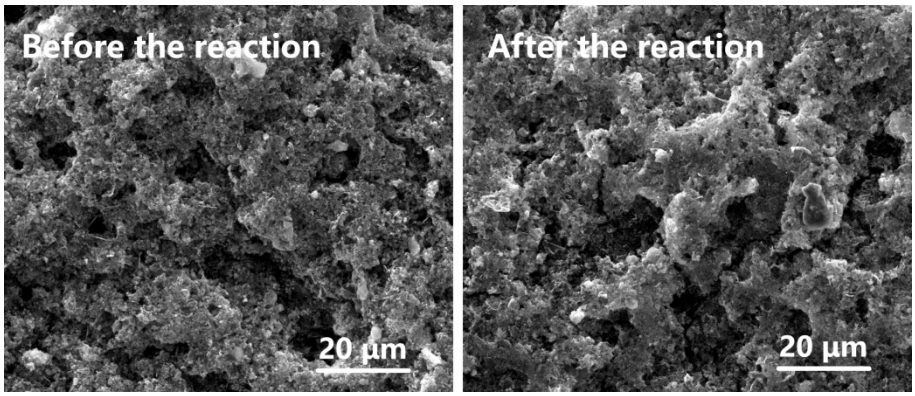

Fig. S12 SEM images of the Cu6/Ni6 electrode before and after the reaction.

XPS and SEM tests were conducted on the Cu6/Ni6 electrodes before and after the reaction. As shown in Fig. S11, the XPS results indicate that the binding energies of C and Ni elements remain almost unchanged, while the binding energy of Cu shifts to the right after the reaction. This shift may suggest a change in the oxidation state of Cu, likely due to its involvement in redox reactions during the catalytic process. Such a change might also be the reason for the decline observed in the stability test. The SEM characterization results (Fig. S12) of the electrodes before and after the reaction show no significant morphological changes, with both exhibiting a uniform and dense porous structure. Based on the above test results, it can be concluded that although the morphology remains stable, the change in chemical

composition (especially of the Cu element) may have an impact on the long - term stability of the electrode.

Table S1. The equivalent circuit fitting results of each group of electrodes

Sample	Rs	CPE-T	CPE-P	Rct	CPE1-T	CPE1-P	R_1	CPE2-T	CPE2-P	R_2
Cu6	0.95	0.02	0.55	7.14	-	-	-	-	-	-
Cu6/Ni1	1.08	-	-	-	0.05	0.43	1.19	0.03	0.85	4.11
Cu6/Ni3	1.06	-	-	-	0.01	0.70	0.65	0.05	0.74	6.37
Cu6/Ni6	1.10	-	-	-	0.04	0.48	0.70	0.11	0.81	2.88

In the journey towards large-scale industrial application, ensuring the scalability of the process and the stability of the catalyst is undoubtedly of vital importance. The following is an in-depth analysis of the process scalability, as well as the potential challenges and corresponding solutions that may be encountered in industrial application.

Judging from the achievements obtained at the laboratory stage, although the indicators such as conversion rate and yield are satisfactory, scalability is the key to moving towards large-scale industrial application. Under the complex scenarios of large-scale production, the catalyst will face a more severe reaction environment, which may significantly accelerate the decline of its activity. Therefore, the stability of the catalyst becomes the core element to realize large-scale expansion. There is a serious problem in the molten salt catalysis process, that is, the condensation of volatile molten salt will cause blockage. To solve this problem, a multi-stage temperature control strategy can be adopted in the reactor design during the process of expanding production scale, to ensure the uniform distribution of temperature, thereby effectively avoiding the blockage caused by the condensation of molten salt.

During the large-scale production process, the generation of waste salt and other waste products is inevitable. How to properly deal with these waste products and prevent environmental pollution is an important problem that needs to be solved urgently. If waste salt can be reused, not only can environmental pollution be avoided, but also resources can be used more efficiently, killing two birds with one stone. For example, waste salt can be used as a high-temperature heat transfer and heat storage medium and added to the molten salt tank of a molten salt solar thermal power station that does not require catalytic action, allowing it to play a role in a new application scenario and achieve the recycling of resources.

References

1 U. Pototschnig, M. Matas, D. Scheiblehner, D. Neuschitzer, R. Obenaus-Emler, H. Antrekowitsch and D. Holec, *J. Phys. Chem. C*, 2024, **128**, 9034-9040.

2 M. A. Abdel-Fatah and A. Amin, *Int. J. Hydrogen Energy*, 2025, **137**, 236-246.

3 S. Musa, B. M. Pirzada, S. H. Talib, D. H. Anjum, M. A. Haija, S. Mohamed and A. Qurashi, *Nano Energy*, 2024, **125**, 109479.

4 M. Cabán-Acevedo, M. L. Stone, J. R. Schmidt, J. G. Thomas, Q. Ding, H.-C. Chang, M.-L. Tsai, J.-H. He and S. Jin, *Nat. Mater.*, 2015, **14**, 1245-1251.

5 J. Sun, F. Tian, F. Yu, Z. Yang, B. Yu, S. Chen, Z. Ren and H. Zhou, *ACS Catal.*, 2020, **10**, 1511-1519.

6 F. Yu, L. Yu, I. K. Mishra, Y. Yu, Z. F. Ren and H. Q. Zhou, *Mater. Today Phys.,* 2018, **7**, 121-138.